Fermi National Accelerator Laboratory

Fermilab-CAIF training course, Summer 2017
Final report

Thermal Chamber Controller for Burn-in System of CMS Silicon Modules

Author:
Tommaso Rizzo

Supervisors:
Anadi Canepa
Lorenzo Uplegger

September 29, 2017

Abstract

My work at Fermilab consisted in the design, development, and testing of the thermal chamber controller for the burn-in system of the new CMS silicon modules.

In the mid 2020s the Large Hadron Collider (LHC) accelerator complex will be upgraded to deliver over 3000 fb^{-1} of proton-proton collision data at 14 TeV with instantaneous luminosities exceeding the nominal one by a factor 5-7. The new machine is referred to as the High-Luminosity LHC, or HL-LHC. To fully exploit the discovery potential of the HL-LHC the CMS detector will be upgraded as well. The upgrade of the current silicon tracker is essential to maintain the capabilities of the CMS detector in the harsh environment expected at the HL-LHC. The new outer tracker (OT) will be capable of providing tracking information to the first-level trigger at 40 MHz for the first time at hadron colliders; furthermore cutting edge technologies are adopted to ensure the longevity and efficient perfomance of both tracker sensors and tracker electronics over the course of the HL-LHC (10 years).

The outer tracker [1] will base its functioning on new silicon modules, that will have to work at temperatures lower than 33 °C to mitigate the effect of high radiation dose. Quality control of the each one of the ∼13,000 OT modules is therefore an integral component of the production phase.

To test the proper working of the silicon modules at low temperatures, Fermilab is developing a burn-in system. A burn-in system is an experimental setup where modules are operated at pre-defined temperatures and humidity levels. This setup must operate un-attended and provide fail-safe modes to reduce risks. My contribution to the project starts here, since I designed and developed the control section of the burn-in system. A Beaglebone Black is the main unit, and monitors the temperature and dew point of the burn-in chamber where the modules will be operated for 24h with temperatures cycling from room to operating temperature. To properly interface with all the silicon modules, I designed an interface board called the *"Burn-in Box Controller Interface"*. The software, written in C++ and integrated in OTSDAQ [2] (the data acquisition software developed by the Fermilab Computing Division), is capable of handling all the critical conditions. Finally, the Beaglebone will be connected to a touch-screen display and provided with a GUI, that will allow a standalone usage alongside a user-friendly interface.

Contents

Chapter 1

Introduction

When I arrived at Fermilab, I had very little background on the CMS experiment at CERN. In this section, I will provide a brief explanation of the Large Hadron Collider and CMS focusing on the outer tracker upgrade.

1.1 LHC upgrade

The LHC [3] is a proton-proton collider currently operating at a center of mass-energy of 13 TeV. Collisions take place at 40 MHz. Four multipurpose experiments are installed along the ring: ALICE, ATLAS, CMS, LHCb. The dataset intially delivered by the LHC and collected by the ATLAS and CMS experiment allowed for the historical discovery of a Higgs boson in 2012. As of today the ATLAS and CMS experiments have collected over $70\,\mathrm{fb}^{-1}$ of data at 13 TeV and operate at peak instanataneous luminosities of $2 \times 10^{34}\,\mathrm{m}^{-2}\,\mathrm{s}^{-1}$. This condition correspond to an average number of interactions per bunch-crossing of 40.

Starting from the mid 2020s, the machine will be upgraded to the HL-LHC. The center of mass-energy of the HL-LHC will be 14 TeV. The peak instantaneous luminosity will exceed $5 - 7 \times 10^{34}\,\mathrm{m}^{-2}\,\mathrm{s}^{-1}$ the nominal one and the collected dataset will be 40 times larger than the current one. The major consequences deriving from this upgrades are the increase of the number of interactions per bunch-crossing to up to 200 (Figure 1.1) and the large dose deposited on the active elements of the detector (10 times more dose with respect to the actual one).

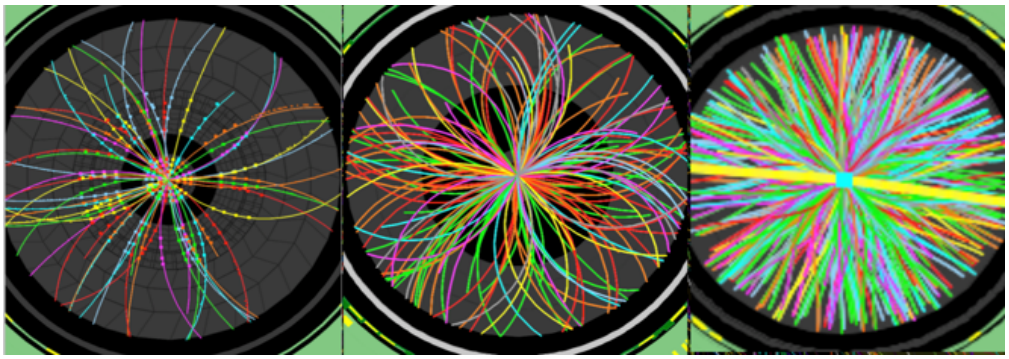

Figure 1.1: Increasing number of collisions-per-bunch crossing in HL-LHC

1.2 What is CMS

CMS [4] stands for Compact Muon Solenoid. It is designed to detect a wide range of particles emerging from the high-energy collisions that happen every 40 MHz in LHC. The different particles are measured and detected by the different sub-detectors of CMS, that are built concentrically around the beam line, like a cylindrical onion.

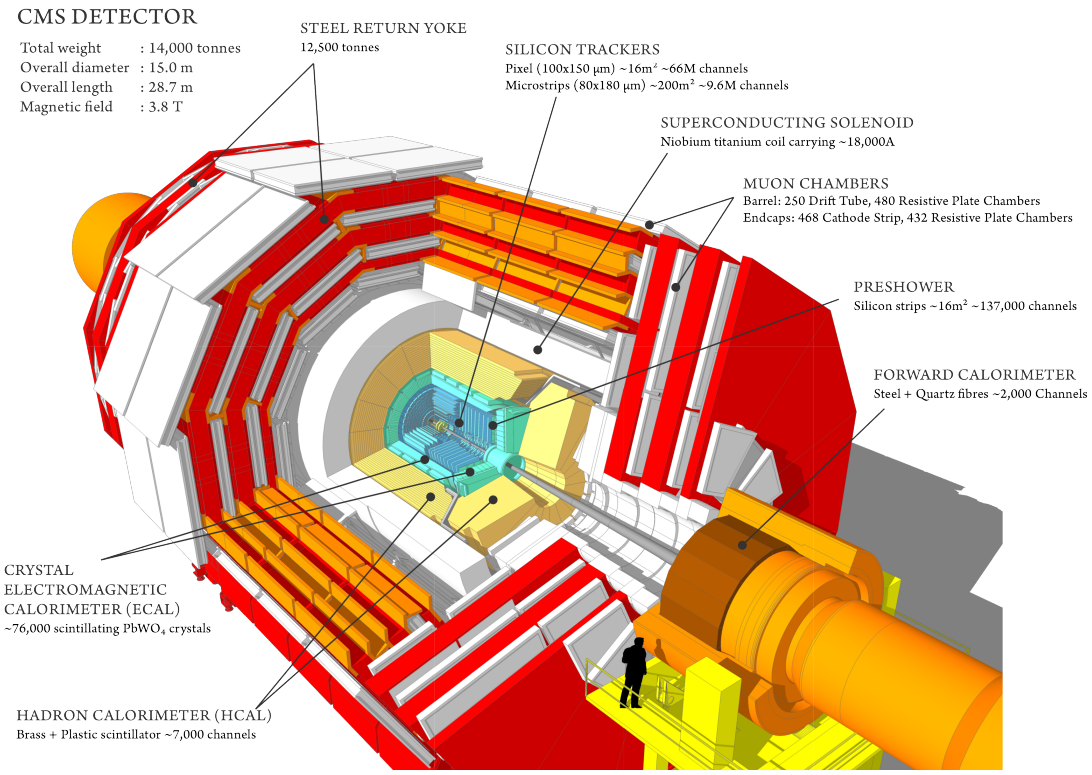

Figure 1.2: CMS detector design

In Figure 1.2 we can see the different sub-detectors with which the various particles are detected: the tracking system gives accurate momentum measurements of charged particles, the electromagnetic calorimeter detects electrons and protons, the hadron calorimeter measures the energy of particles undergoing hadronic interactions, the muon chamber detects muons.

To cope with the higher number of interactions per bunch-crossing and the large doses expected from the HL-LHC, the CMS detector must be upgraded. For these reasons, CMS will build a new outer tracker that will have:

- High granularity sensors to separate closed-by-charged particles events.
- Radiation hard sensors and radiation hard front-end electronics.

But the biggest innovation in the upgraded tracker will be the capability to provide tracking information at the machines' frequency, 40 MHz, to the level-one trigger level. This is essential to maintain high purity and low rate trigger operations and thus to collect relevant collisions efficiently.

1.3 CMS outer tracker

As previously said, the new outer tracker (Figure 1.3) will have radiation hard sensors to cope with a higher radiation dose with respect to the current tracker; since the front-end electronics will have to be radiation hard as well, it will mostly be digital for its better hardness compared to analog front-ends.

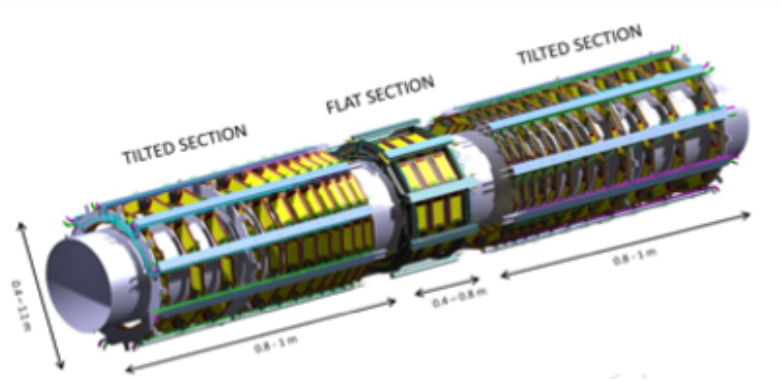

Figure 1.3: 3D model viewing of the new CMS outer tracker

The main elements of the outer tracker will be the new **silicon modules**, that will be presented in Chapter 2. They will be assembled from two silicon sensors. The sensors will contain either strip-like implants or pixel-like implants. There will be two kind of modules, depending on its sensors: strip−strip (2S) and macro-pixel−strip (PS).

	Current	Phase 2	
Silicon [m^2]	200	220	Outer tracker
Strips	9×10^6	48×10^6	
Macropixels	–	217×10^6	
Modules	15 148	15 508	
Readout rate [kHz]	100	750	
Stub readout rate [kHz]	–	40 000	

Table 1.1: Comparison between current tracker and new outer tracker (the most recent OT channel count will be made public in the upcoming Technical Design Report).

Table 1.1 highlights the main differences between the new outer tracker and the current one. Two are the features that mainly stand out:

1. new outer tracker will have around 30 times more channel than the current one, thanks to the increased numbers of strips and the addition of nearly 300 millions of pixels,

2. it will be capable of giving a measurement − transverse momentum − of charged particles, in situ, at 40 MHz.

Figure 1.4 shows a quarter view of the OT. The z-axis represents the direction of the beams. The modules are placed in 6 layers around the z-axis, while 5 barrel layers are placed perpendicularly in the end-cap region. The numbers represent the distance

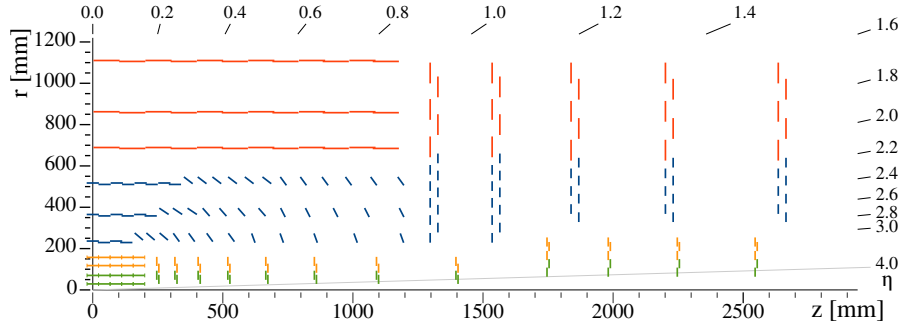

Figure 1.4: Outer tracker section view (the most recent OT layout will be made public in the upcoming Technical Design Report). Sketch of one quarter of the tracker layout in r-z view. In the Inner Tracker the green lines correspond to pixel modules made of two readout chips and the yellow lines to pixel modules with four readout chips. In the Outer Tracker the blue and red lines represent the two types of modules described in the text.

between the two sensors of each module: this distance is optimized by how far the modules are from the interaction vertex typically located in the origin of the axes. Modules in the central region at large z are inclined to ensure normal incidents of particles emerging from the interaction vertex.

Chapter 2

Outer tracker modules

2.1 General Description

As previously mentioned, each module is assembled from two silicon sensors. Each sensor can be made out of strips or macropixels, and the modules are built in two configuration:

- Strip−Strip (2S)
- Pixel−Strip (PS)

The main idea behind the modules is that they are constituted by two sensors physically separated by a few millimeters, but still they are read out by the same electronic circuits. This allows them to make measurements, in situ, at 40 MHz, and send them to CMS Level 1 trigger.

Figure 2.1 shows how the silicon modules work. They are separated by a distance of $1 \div 4$ mm, depending on the module position with respect to the vertex.

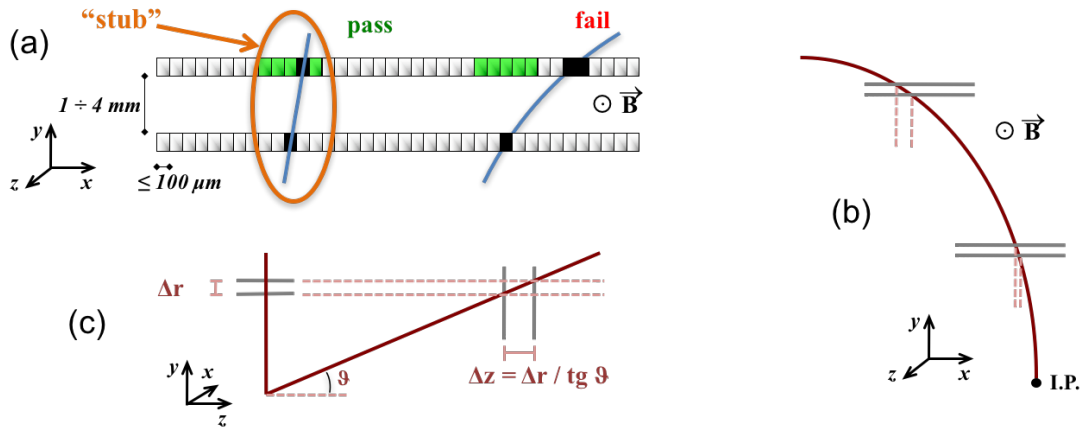

Figure 2.1: Illustration of the module concept. (a) Correlation of signals in closely-spaced sensors enables rejection of low-particles; the channels shown in green represent the selection window to define an accepted stub. (b) The same transverse momentum corresponds to a larger distance between the two signals at large radii for a given sensor spacing. (c) For the endcap discs, a larger spacing between the sensors is needed to achieve the same discriminating power as in the barrel at the same radius.

The high CMS magnetic field (3.8 T) allows to measure the transverse momentum p_T of charged particles by correlating the hit on the bottom to the hit on the top sensors. In fact, transverse momentum is proportional to the inverse of the curvature of the charged particles:

$$p_T = 0.3 \times \frac{B}{C} \propto \frac{1}{C}$$

Definition (stub): *A* stub *occurs every time the hit on the bottom matches with the hit on the top (with a variance represented by the green channels as shown in Figure 2.1a): the signal of the match is sent by the electronic front-end to L1 trigger.*

The modules are optimized to measure charged particles with $p_T > 2\,\text{GeV}$.

As will be explained in Section 2.3, the modules will need to run at very low temperatures – about $-33\,°\text{C}$ – for proper working.

2.2 Geometry

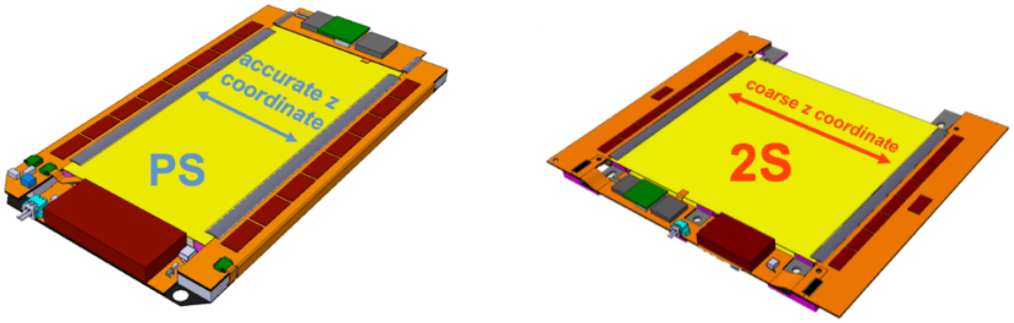

Figure 2.2: 3D model for the PS and 2S silicon modules

Figure 2.2 and Table 2.1 show the geometric features of the silicon modules. It is important to highlight the pitch – 90 µm for the 2S and 100 µm for the PS –, the number of pixels/strips in each module, and their active area: the 2S will have a squared shape of $10 \times 10\,\text{cm}$, while the PS will be a rectangular of $10 \times 5\,\text{cm}$.

	PS	2S
Strips	2×960	2×1096
Pixels	32×960	–
Pitch	100 µm	90 µm
Length	strips:$\sim 2.5\,\text{cm}$ pixels:$\sim 1.5\,\text{cm}$	$\sim 2.5\,\text{cm}$
Active area	$\sim 50\,\text{cm}^2$	$\sim 100\,\text{cm}^2$

Table 2.1: Characteristics of the modules

2.3 Silicon sensors working principles

The two silicon sensors which compose each module are a reversed biased n-in-p junction. In this way, the bulk region is completely depleted of free charged carriers. When the charged particle passes through the junction after the collision, it leaves a track by creating an electron-hole pairs. The electrons drift to the anode and generate the signal.

The problem comes with the high radiation dose and high fluence to which the sensors will be exposed during the data taking. In order to have them work properly until the end of the project, the only solution is to work at a **low operating temperature**.

In fact, the sensors leakage current I_{leak} is directly proportional to the temperature from the relation

$$I_{leak} \propto T^{3/2} e^{-E_g/kT}$$

and while the inverse biasing lowers the I_{leak}, when exposed to radiation its value increases according to the formula and can bring to **thermal runaway** if the proper temperature is not maintained. Figure 2.3 reports this phenomenon, showing the relation between $T^{max}_{sensor} - T_{CO_2}$ and T_{CO_2} itself (T_{CO_2} represents the operating temperature since the cooling system is based on evaporative CO_2).

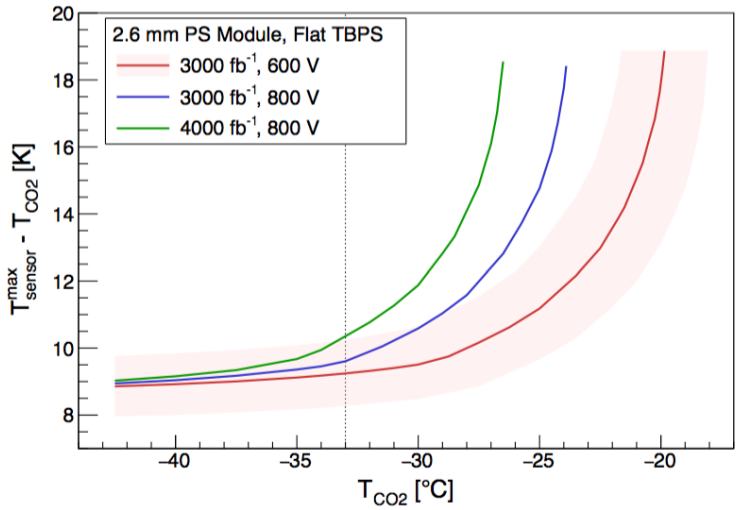

Figure 2.3: Thermal Runaway

If the operating temperature is not kept around $-33\,°C$, thermal runaway occurs and the junction fails.

Chapter 3

Burn-in System Overview

In Chapter 2 have been described the principles of the outer tracker modules, and has been highlighted that they have to run at low temperature for proper functioning.

Therefore, quality control is critical to ensure that they will work for the entire duration of the project (around 10 years) at the operating temperature: every module has to be suitably tested prior to assembling.

In order to do this, Fermilab is developing a Burn-in System to properly test the modules. The tests will be made while irradiating and reading the modules, at operating temperature.

Finally, the Burn-in System will be produced and distributed in every CMS module production center in the World.

3.1 Burn-in System Description

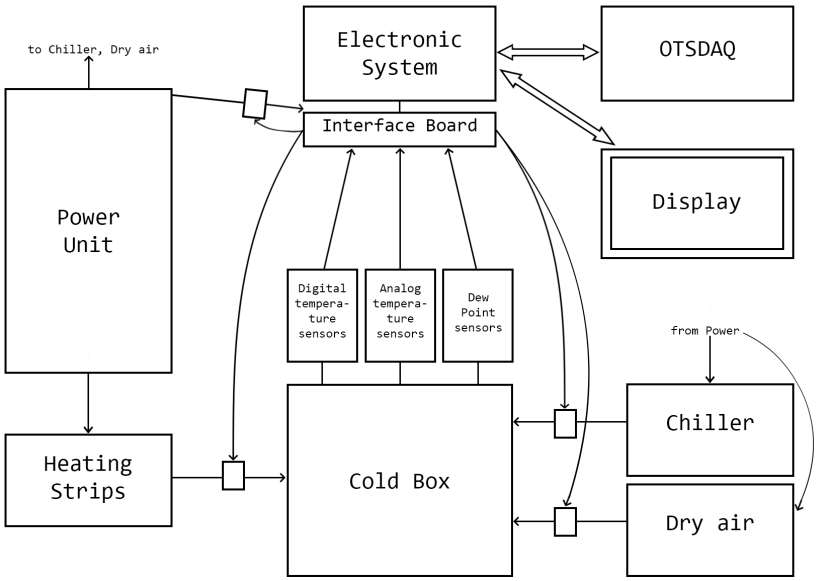

Figure 3.1: Burn-in System Block Diagram

Figure 3.1 shows the overview of the entire system.

The modules will be tested in the *Cold Box*, that is linked to the *Chiller* and the *Heating Strips*, responsible for lowering or increasing the temperature of the box, and to the *Dry air supply*, that controls the humidity value.

The *Electronic System* is the main core of the system: its task is to monitor temperature and dew point of the box by reading all the various sensors through the *Interface Board*, and to activate/deactivate chiller, heating strips, dry air by using relays (switches) represented by the small rectangles. The relays are also used as a safety feature, since they can activate the various machines to re-estabilish the proper temperature and humidity values if something is wrong. The Electronic System will have the possibility to be controlled by two different softwares:

- one integrated with Off The Shelf DAQ (*OTSDAQ*), which is the data acquisition software that will be used for the outer tracker, developed by Feynman Computing Division at Fermilab;
- the second will be running directly on the Electronic System, which will be linked a *Display* for local standalone usage.

Finally, The *Power Unit* will provide power to all components.

The tests will last 24 hours, with 4/5 cycles from operating to room temperature.

One of the main features of the Burn-in system will be the capability of operating **un-attended** for the entire duration of the tests.

3.2 Cold Box

Ten silicon modules will be tested inside the thermally insulated Cold Box (Figure 3.2). The cooling system is based on peltiers, and a clamping mechanism ensures the thermal contact with the modules. Each module will consume, after irradiation, around 10 W of power (2S: $\sim$ 6 W, PS: $\sim$ 9 W). Given that the power consumption is dominiated the by the front-end electronics this estimate is adopted as the requirement for the cooling system.

The box has been developed at Silicon Detector Facility at Fermilab.

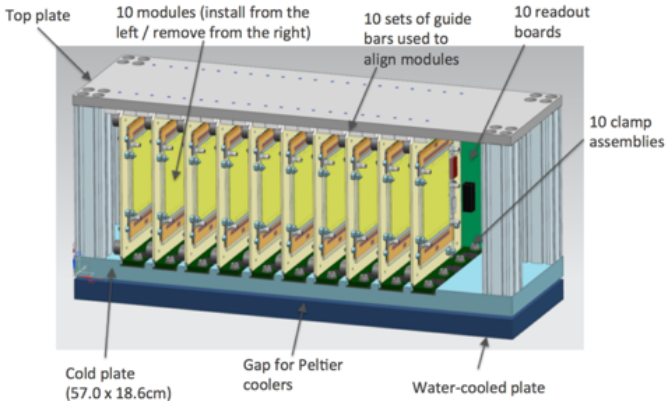

Figure 3.2: Cold Box Mechanical Design

Chapter 4

Electronic Control System

In this Chapter I am going to present what has been my contribution to the Burn-in System: my task, in fact, was to define the entire Electronic Control System, developing the hardware to control all the different components and writing the software for its functioning. I divided my work in four main parts:

1. choice of the device for the Electronic System;
2. choice and testing of the humidity and temperature sensors and relays;
3. design, production and assessment of an Interface Board;
4. design and development of the software integrated with OTSDAQ.

4.1 Main Device

After having considered different options, the device that was chosen is a **Beaglebone Black** (BB), a commercial electronic board that runs Debian Linux OS (Figure 4.1).

Beaglebone Black (`https://beagleboard.org/black`) was compared to other electronic boards and similar devices, but it has been chosen as it offers:

- high number of I/O ports (more than 70), that allow to connect a large number of sensors;
- availability of 7 1.8 V Analog Inputs for an immediate connection of the analog sensors that are needed;
- powerful CPU and Linux OS allow to exploit the potentialities of C++ software.
- Ethernet port that allow SSH access through local network;
- HDMI port to connect to a display for standalone usage.

The task of the Electronic System is to monitor the temperature and dew point of the cold box where the modules will be installed and tested.

It is necessary to monitor the temperature and keep it within a few degrees with respect to the nominal one to avoid thermal runaway (*cf. Chapter 2, section 2.3*). Dew point monitoring is instead needed to avoid condensation that would damage the wire-bonds of the modules, for example.

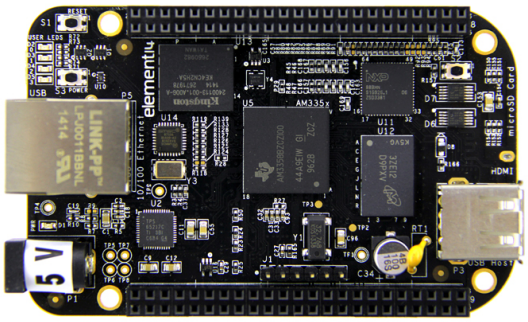

Figure 4.1: View from the top of the electronic commercial board Beaglebone Black. On the sides it is possible to see the two 2×23 header for the I/O pins. USB, Ethernet and HDMI ports are available too. Through the 5 V connector, power its provided to the whole device.

Therefore, an important part of the job has been the choice of the suitable temperature and dew point sensors, together with the relays for fail-safe mode.

4.2 Device Testing

After an accurate research and proper testing, the sensors and relays that have been chosen are summarized in the following list:

- **10 digital temperature sensors**, that will be placed near to each module to monitor their temperature.
- **3 analog temperature sensors**, that will monitor the temperature of the entire cold box. They will be used for safety failure mode due to their fast response time.
- **2 analog dew point sensors**, tracking the dew point if the box.
- **6 digital solid state relays**, used to activate and de-activate all the components of the Burn-In System (Chiller, Dry Air, Heating Strips...).

4.2.1 Digital Temperature Sensors

The digital temperature sensors chosen are the DS18B20 [5].

Their most important feature is that they communicate via a **1-wire connection**: by configuring a Beaglebone I/O pin with a 1-wire interface, it is possible to connect all the sensors to that same pin and easily read their measurement through a file in BB memory.

Therefore, 10 digital sensors will be used in the cold box, placed close to each module to monitor their temperature, with a requirement of $\pm 1\,^{\circ}\mathrm{C}$ accuracy at the operating temperature.

The datasheet indicates an operating range of the sensor of -55 to $125\,^{\circ}\mathrm{C}$, with an accuracy of $\pm 0.5\,^{\circ}\mathrm{C}$ only in the range $[-10, 85]\,^{\circ}\mathrm{C}$.

In order to calibrate the sensors and verify their accuracy at operating temperature of $-33\,°C$, test were made at low temperatures.

The sensors have 3 wires: power, ground and data. As in Figure 4.2a, the data of each of the 4 sensor used was connected to the same Beagelbone I/O pin; power was provided by BB 3.3 V pin, and a $4.7\,k\Omega$ pull-up resistor was placed between the data wire and power. The Beaglebone was accessed via SSH and its I/O pin configured to read the measurements from each sensor and store them in a .csv file.

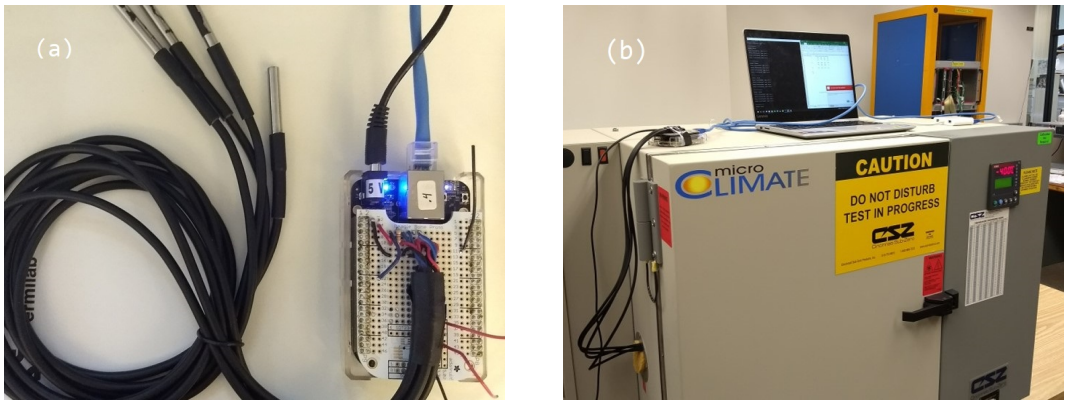

Figure 4.2: DS18B20 sensors testing. (a) Connection to Beaglebone (b) Insertion in thermal chamber.

The 4 sensors were then placed inside the *microClimate Thermal Chamber*, available at Feynman Center at Fermilab, through a hole on the side (Figure 4.2b).

The procedure for the data taking consisted in: setting the thermal chamber temperature and waiting for it to stabilize; taking 2×10 measurements, one every 5 seconds, for each sensor at each temperature. Measurements were then processed and results are shown in Table 4.1.

Thermal Machine Temp. [°C]	Average Temp. of Sensors [°C]
-30	-29.208 ± 0.115
-35	-33.993 ± 0.183
-40	-38.762 ± 0.120
-45	-43.781 ± 0.114

Table 4.1: Results of digital sensors DS18B20 testing at low temperature. The average temperature is the average of the average measurement of each sensors at the specified temperature. The accuracy is the average of the standard deviation for each sensor.

Th results point out two kind of errors:

- a **statistical uncertainty**, represented by the standard deviation, due to the normal difference between the sensors and between the various measurements: it is very low (always $< 0.2\,°C$) and consistent;
- a **systematic uncertainty** of about $1\,°C$. This offset can depend on different factors such as sensors aging, machine miscalibration, temperature gradient in the

chamber, and therefore does not affect the correct functioning of the sensors.

In conclusion, the results were considered satisfactory and the accuracy qualification was passed.

4.2.2 Analog Temperature Sensors

The choice of using 3 additional temperature sensors was made because of the slow response time of the DS18B20 sensors, that makes them not suitable to handle safety-failure cases. For these reason, the OMEGA SA1-RTD [6] are introduced: they are PT100 RTDs with high precision temperature measurement (accuracy $< 0.35\,°\text{C}$ at $-33\,°\text{C}$) and response time lower than 1 second.

Definition (RTD): *A RTD (resistance temperature detector) is a resistor which varies its value according to its temperature. The temperature coefficient of resistance (α) is given by:*

$$\alpha = \frac{R_{100} - R_0}{100\,°\text{C} \cdot R_0}$$

If the RTD is a PT100, the values for R_0 and α are:

$$\begin{cases} R_0 = 100\,\Omega \quad \text{resistance at } 0\,°\text{C} \\ \alpha = 0.003\,85\,\Omega/(\Omega\,°\text{C}) \end{cases}$$

Additional circuitry is needed to connect the RTD to the analog input of BB, since they are resistors and the analog pins only accept voltages in the range $[0, 1.8]\,\text{V}$. After testing different solution, the electronic circuit chosen is the one shown in Figure 4.3, which uses 0.05% tolerance resistors and high precision amplifiers. The $V_{U1}^{+} = 1.8\,\text{V}$ is taken from the VDD_ADC pin on Beaglebone, and is a precise voltage reference ($\pm 2\,\text{mV}$), while the two amplifiers are powered by the same $5\,\text{V}$ supply that powers BB.

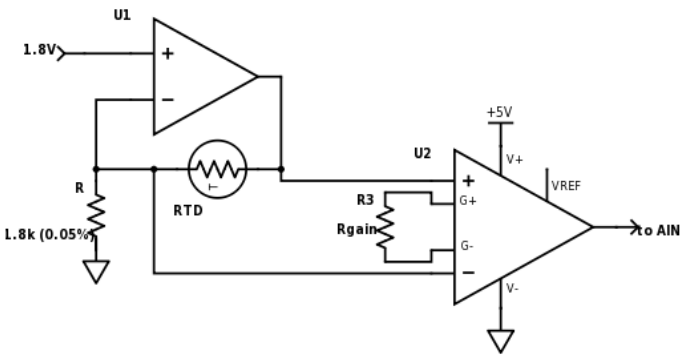

Figure 4.3: Electronic scheme for RTD sensor connection to BB analog input. U1 is an op-amp in the V-I converter configuration that, together with R, make a 1 mA current flow in the RTD. The voltage dropped on the RTD is then amplified by the in-amp U2 that adjusts the voltage range for connection to the analog input.

The current value of 1 mA is chosen to minimize the error due to the self-heating of the RTD. From the conversion tables [7], at 80 °C (maximum temperature possible) the

resistance value is $130.90\,\Omega$ and thus the input voltage of the in-amp is:

$$130.90\,\Omega \cdot 1\,\text{mA} = 130.90\,\text{mV}$$

In order to adjust the voltage range, the gain − set by R_{gain} − should be:

$$G = \frac{V_{ADC}^{MAX}}{V_{in}^{MAX}} = \frac{1800}{130.90} \simeq 13\,\text{V/V}$$

This circuit was tested on a breadboard with 1% tolerance resistor and three op-amps that emulated the behavior of the in-amp. Figure 4.4 shows the setup. The RTD sensor was connected to the BB analog input and accuracy and response time were tested via software: even with this rough circuit, results were satisfactory.

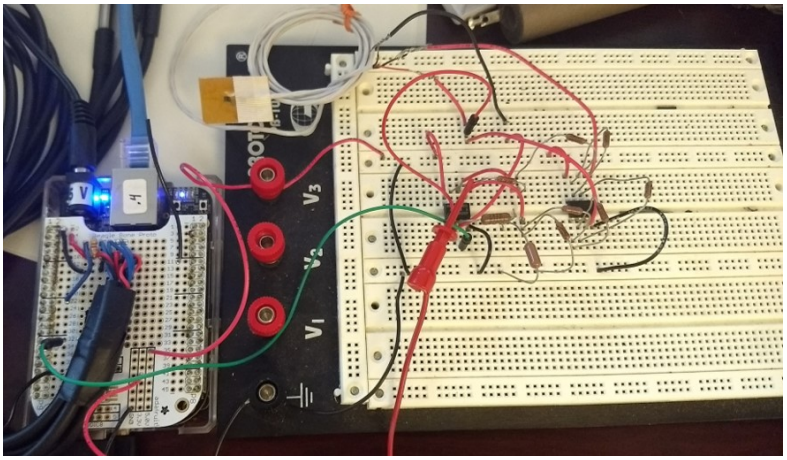

Figure 4.4: Testing setup for the RTD sensor. The two integrated circuits are multicomponent operational amplifiers (each IC has 2 op-amps). The black component connected to the white wires is the RTD.

4.2.3 Analog Dew Point Sensors

Dew point sensors are needed to monitor the dew point of the chamber, with a few %RH accuracy and fast response time.

After proper testing two sensors were chosen as suitable for the application: VAISALA DMT143 [8] (Figure 4.5a) and TE HTM2500LF [9] (Figure 4.5b).

One of the DMT143 output is a 4 to 20 mA analog output that can easily be converted to a voltage by using a $90\,\Omega$ resistor between it and the analog input of BB.

The sensor was tested first using a digital display produced by Nokeval and then connecting the output to the analog input of BB. As from datasheet, results showed an accuracy on dew point temperature lower than 2 °C, completely acceptable. The cons of this sensor are primarily represented by its high cost.

The HTM2500LF has two output channels, one for humidity (0−4 V) and one for temperature (NTC − Negative Temperature Coefficient − resistor). The humidity can be measured by putting a voltage divider before connection to the analog input; a NTC is a resistor that lowers its value with the temperature: it is less precise than a RTD

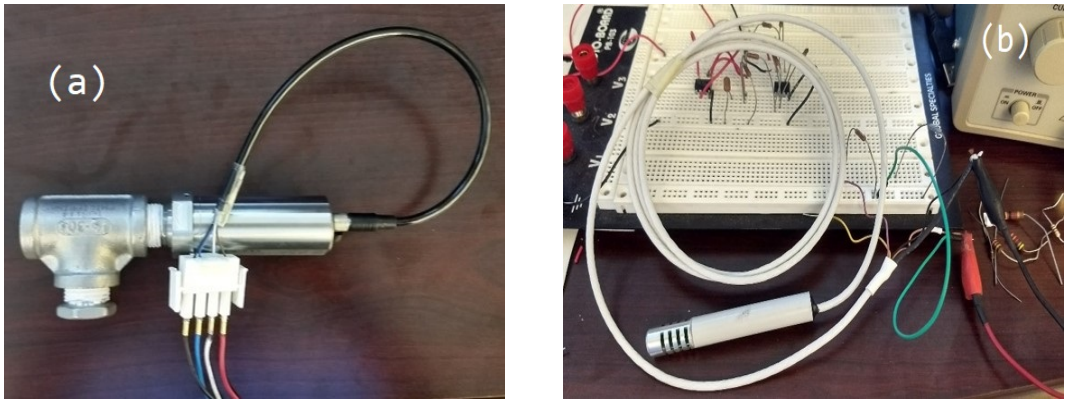

Figure 4.5: Dew point sensors. (a) DMT143 analog output gives the direct measurement of the dew point. Its 4 wires are: power, ground, and two channels for measurement. (b) HTM2500LF has two analog outputs that give the measurement of humidity and temperature, coming out from 2 wires. The other 2 are for power and ground.

and so does not require a high precision circuit. It is sufficient to use a pull up resistor to 1.8 V and read the voltage dropped on the NTC to get the measurement.

Tests showed an accuracy on humidity of $\pm$ 3 %RH, worse than the other sensor; on the other hand, the HTM2500LF has a significantly lower cost.

4.2.4 Digital Solid State Relays

The solid state relays (SSR) have the function to turn on and off the various component of the Burn-in system. They will therefore be used for both normal operation (activating the dry air and the chiller to reach and maintain operating temperature and dew point) and fail-safe mode (turning on the dry air if the dew point value increases significantly, for example).

SSRs have 2 channels for the input (IN+ and IN-) and 2 channels for the load: in order to test them, they had to be connected to the load since they require power to work correctly.

They were tested by connecting IN- to ground and IN+ to 0-3.3 V I/O pins, and by connecting the load channels to:

- a lamp and a 120VAC power supply to test the relays for the heating strips (that need 120VAC power);
- a LED in series to a resistor in series to a 24VDC power supply to test the relays for the other components, that need 24VDC power.

Results showed that BB could perfectly control the SSR, that turned on and off the lamp or the LED depending on the input.

4.3 Interface Board

After having selected and tested all the sensors, the problem was their proper connection to the Beaglebone.

So, I designed, developed and then produced an **Interface Board** for the electronic system, on which there would be all the connectors for the sensors, relays, and the Beaglebone itself, together with the circuitry needed for correct functioning.

4.3.1 Electric Scheme

I designed the electric scheme using KiCAD EDA™software, an open-source software for schematic and PCB design available also for Linux. The entire schematic is shown in the Appendix.

Figure 4.6 shows a part of the scheme that represents the final circuit used for the RTD sensors. In addition to the one shown in Section 4.2.2, there are:

- capacitors $C_{10}, \ldots, C_{13}$ together with $R_{13}, \ldots, R_{16}$, make an anti-aliasing low-pass filter prior connection to BB's ADC pins;
- bypass capacitors for both the op-amp and in-amps;
- gain is set by R_5 and $R_9, \ldots, R_8$ and R_{12} according to the equation (given by the in-amp datasheet):

$$G = 2 \cdot \frac{200\text{k}}{29.4\text{k}} = 13.60\,\text{V/V}$$

Power to the Interface Board is brought by a 24VDC connector (since the DMT143 dew point sensors requires 24VDC) and converted to 5 V that powers Beaglebone and the remaining sensors through a DC-DC switching converter shown in Figure 4.7.

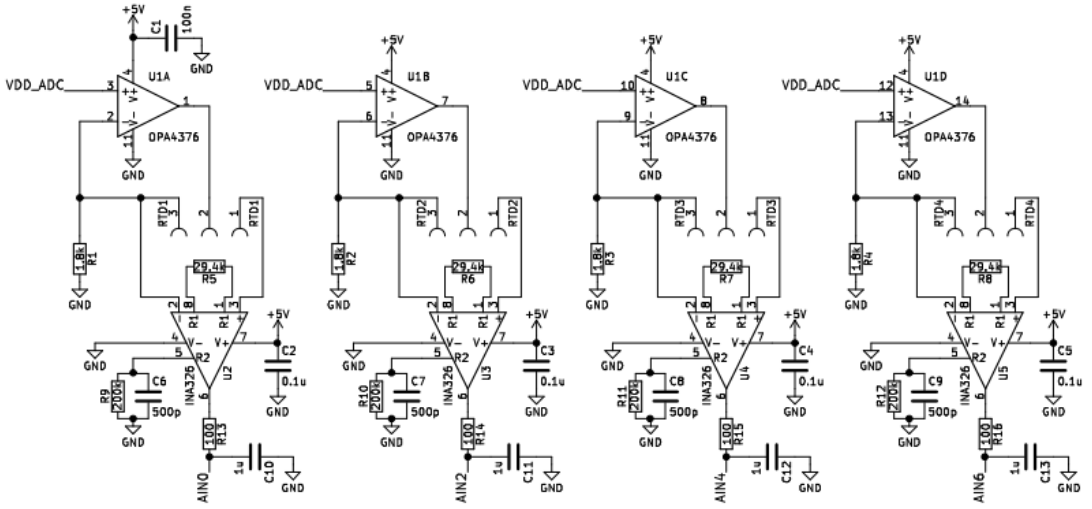

Figure 4.6: Electric scheme for the RTD sensors' interface with BB. On the Interface Board there are four connectors to connect up to four RTD sensors.

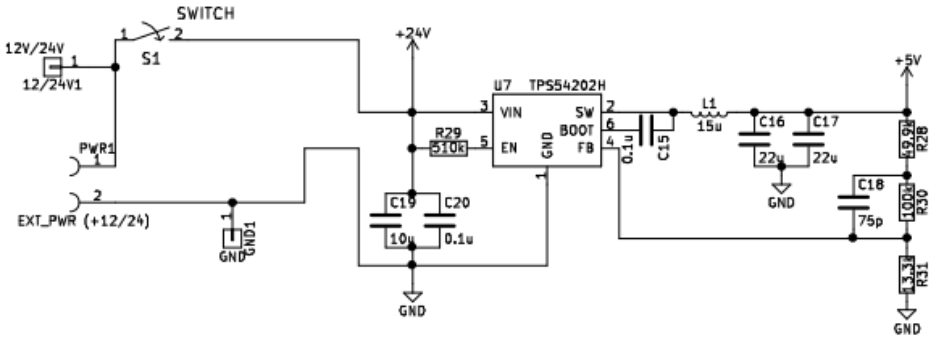

Figure 4.7: Electric scheme for the DC-DC converter. It can take as input voltages from 4.5 to 28 V and deliver up to 2 A current. The output voltage is set by the three resistors R_{28}, R_{30}, R_{31}.

4.3.2 Printed Cricuit Board

I designed the physical layout for the Interface Board, the **"Burn-In Box Controller Interface"** (Figure 4.8), using the KiCAD software that also allows to design printed circuit boards. Its specifications are the following:

- dimensions: 13×13 cm;
- 4 layers
  - Front and Back Copper;
  - GND;
  - PWR (5 V).
- tracks: $0.25 \div 1.5$ mm;
- vias: 30 mils diameter, 15mils drill.

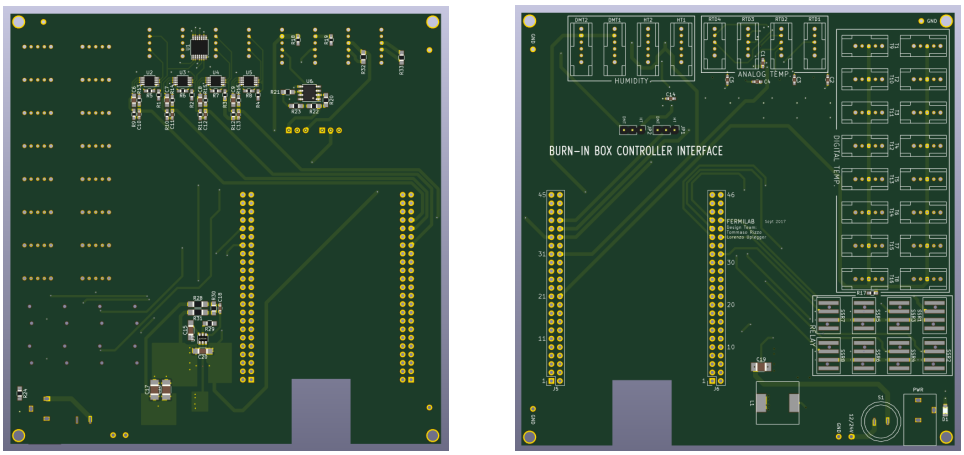

Figure 4.8: Front and back faces of the Interface Board shown with KiCAD 3D viewer

Prior to production, the board underwent a formal technical review within the Scientific Computing Division at Feynman Center. Five boards arrived in mid-September and I spent the last weeks debugging and testing them. Figure 4.9 shows the finished product under debugging.

The Burn-In Box Controller Interface will be produced for all CMS centers where the Burn-in system will be used.

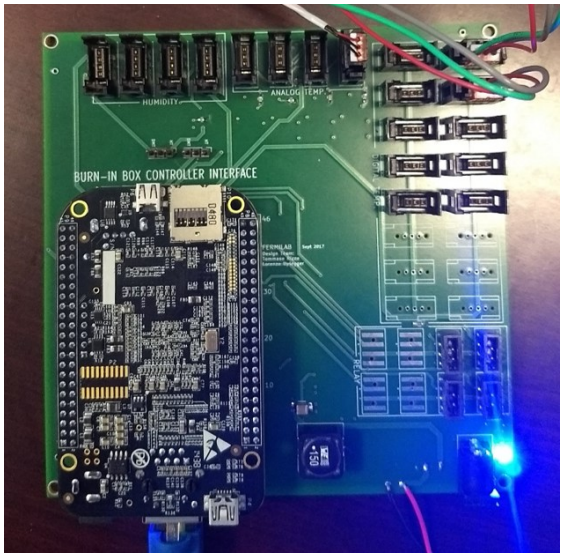

Figure 4.9: Soldered "Burn-In Box Controller Interface" with Beaglebone and selected sensors at the debugging phase.

4.4 Logic Implementation

After having defined all the hardware (main unit, sensors and relays, Interface Board) and prior to writing the code, the logic implementation of the Control System was defined. The normal operation is divided into three phases.

1. Start:
    - activate, using the corresponding relays, the dry air supply until dew point is under critical value;
    - activate chiller until desired temperature is set;
    - repeat the previous steps until operating temperature and dew point are reached.
2. Data Acquisition (run):
    - use relays to mantain temperature within $\pm 1\,^{\circ}\mathrm{C}$ with respect of desired one;
    - always check if modules temperature is safely above dew point.
3. Stop:
    - activate heating strips until room temperature is reached;

- turn off power.

Two types of failures/faults have been highlighted:

1. failure handling: chiller, heating strips, dry air machine will be properly turned on/off when critical values are reached;
2. fault handling: relay will turn off power if un-solvable situation is faced.

4.5 Software

The software will ultimately allow to run ther system either in a standalone manner or through OTSDAQ.

My responsibility was to develop the software integrated into OTSDAQ. In this case the interface on the PC controller is set as a UDP communication.

The control software that runs on Beaglebone generates a class for every sensor connected to the board: since Linux OS interprets the inputs as an internal file, each class has its proprietary method to read the related file and return the measurements of the device.

4.5.1 Device Mapping

Figure 4.10 shows how the device mapping is implemented in the software. The device class takes the information both from the file, created by Linux on Beaglebone every time the I/O pin is configured, and from an additional .xml file, created on BB, which contains all the information of every device used, such as category, name, type, status and path.

In particular the status (*on* or *off*), indicates whether the device is being used by the system or not: the software takes this information and decides whether that specific device should be considered or not, even if it is physically connected to the Interface Board.

Figure 4.10: Scheme for device mapping on C++ software

The "Device Mapping" class gathers all the information from the two files and creates a class object for each device:

```
new Device(name, status, path);
```

4.5.2 Device Classes

Figure 4.11 shows the device classes of the software.

The mother class is the "Device" class, from which the various sub-classes inherit the basic information.

"Temperature Sensor" and "Dew Point Sensor" are virtual classes that only define the *readTemperature* and *readDewPoint* functions, which will be implemented by the corresponding class.

Since there are different analog sensors, whose corresponding pins are read the same way, the "Analog Sensor" defines the *readValue* method that is necessary for the heir classes to read the measurement from the sensors correctly.

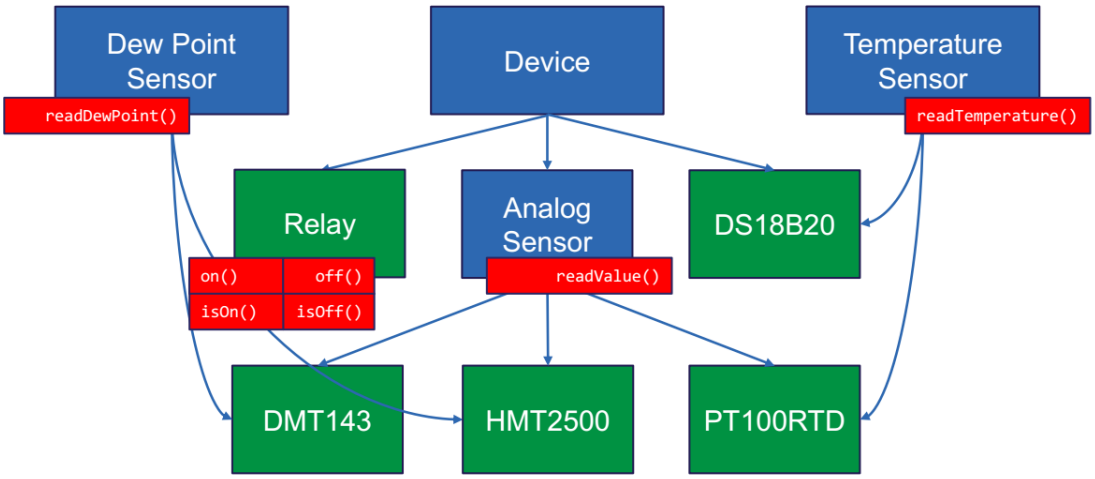

Figure 4.11: Summary of the classes implemented in the C++ software. The ones in green are the classes in which the physical device is mapped.

The reason why such a complex and complicated structure has been developed is that the software will used by the various module production centers; for this reason it has to be user-friendly and easily configurable by those who have not worked on it.

Chapter 5

Conclusions

By the end of my time at Fermilab I completed the project I was assigned: I designed and produced the electronic control system for the burn-in system of the outer tracker silicon modules. In particular:

- I selected and tested all temperature and humidity sensors, together with solid state relays;
- I learned how to control the Beaglebone and to configure the Linux OS on it;
- I designed the Interface Board which has been produced and is now ready to be used;
- I wrote (and learned a lot) C++ software to control the system from OTSDAQ.

Future steps include: the development of the web server and the GUI on the Beaglebone for standalone usage (the touch-screen display has already been selected); a second review of the "Burn-In Box Control Interface": first corrections have already been implemented during the debug phase, however further analysis is expected prior to producing the final version.
And finally, the whole system has to be tested when the modules arrive, prior to production.

I would like to thank all the people that allowed me to have such a great experience and the people that helped me live it in this way.
In particular, special thanks go to my supervisors, Anadi Canepa and Lorenzo Uplegger, for dedicating a lot of time and showing to me their great passion; to the Feynman Computing Division, for all the help I received; to my home, for supporting me from far away; to the new friends I met here, for the time we spent together and for making this experience unique.

References

[1] D Contardo et al. *Technical Proposal for the Phase-II Upgrade of the CMS Detector*. Tech. rep. CERN-LHCC-2015-010. LHCC-P-008. CMS-TDR-15-02. Geneva, June 2015. URL: https://cds.cern.ch/record/2020886.

[2] Feynman Computing Division at Fermilab. *Off The Shelf DAQ*. URL: http://otsdaq.fnal.gov/sandbox/index.php.

[3] *The High Luminosity LHC*. URL: https://home.cern/topics/high-luminosity-lhc.

[4] *What is CMS?* URL: http://cms.web.cern.ch/news/what-cms.

[5] *Programmable Resolution 1-Wire Digital Thermometer*. DS18B20. Maxim Integrated. 2015. URL: https://datasheets.maximintegrated.com/en/ds/DS18B20.pdf.

[6] *Self-Adhesive RTD sensor*. SA1-RTD. Omega Engineering, Inc. 2008. URL: https://www.omega.com/Manuals/manualpdf/M0503C.pdf.

[7] *RTD Temperature vs. Resistance Table*. Omega Engineering, Inc. URL: https://www.omega.com/techref/pdf/z252-254.pdf.

[8] *Miniature Dewpoint Transmitter for OEM Applications*. DMT143. Vaisala. 2015. URL: https://www.vaisala.com/sites/default/files/documents/CEN-G-DMT143-Datasheet-EN.pdf.

[9] *Temperature and Relative Humidity Module*. HTM2500LF. Rev. C. TE Connectivity. 2015. URL: http://www.te.com/commerce/DocumentDelivery/DDEController?Action=showdoc&DocId=Data+Sheet%7FHPC169_C%7FA%7Fpdf%7FEnglish%7FENG_DS_HPC169_C_A.pdf%7FCAT-HSA0001.

List of Figures

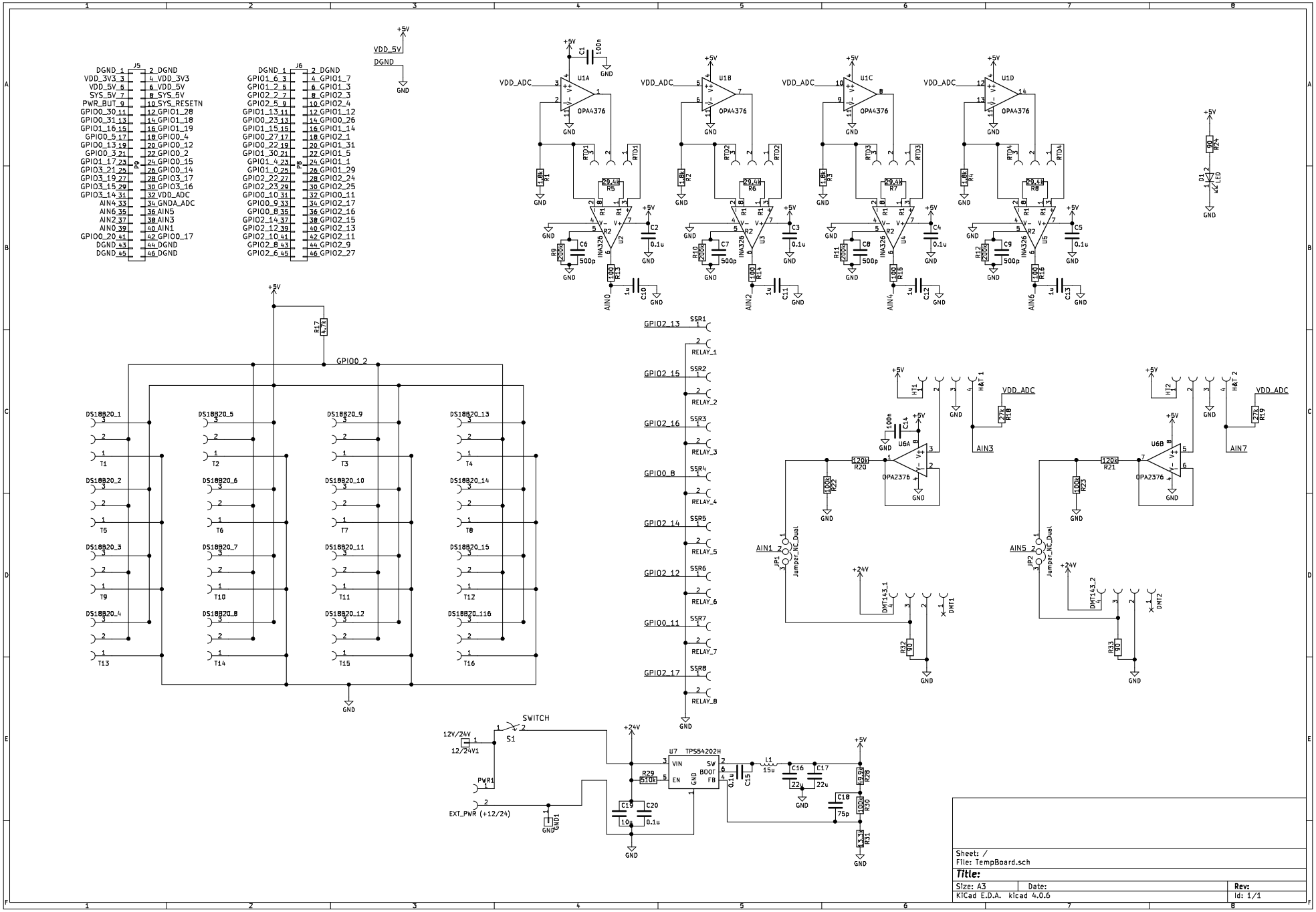
J5
DGND 1
VDD_3V3 3
VDD_5V 5
SYS_5V 7
PWR_BUT 9
GPIO0_30 11
GPIO0_31 13
GPIO1_16 15
GPIO0_5 17
GPIO0_13 19
GPIO0_3 21
GPIO1_17 23
GPIO3_21 25
GPIO3_19 27
GPIO3_15 29
GPIO3_14 31
AIN4 33
AIN6 35
AIN2 37
AIN0 39
GPIO0_20 41
DGND 43
DGND 45
2 DGND
4 VDD_3V3
6 VDD_5V
8 SYS_5V
10 SYS_RESETN
12 GPIO1_28
14 GPIO1_18
16 GPIO1_19
18 GPIO0_4
20 GPIO0_12
22 GPIO0_2
24 GPIO0_15
26 GPIO0_14
28 GPIO3_17
30 GPIO3_16
32 VDD_ADC
34 GNDA_ADC
36 AIN5
38 AIN3
40 AIN1
42 GPIO0_17
44 DGND
46 DGND
P9
J6
DGND 1
GPIO1_6 3
GPIO1_2 5
GPIO2_2 7
GPIO2_5 9
GPIO1_13 11
GPIO0_23 13
GPIO1_15 15
GPIO0_27 17
GPIO0_22 19
GPIO1_30 21
GPIO1_4 23
GPIO1_0 25
GPIO2_22 27
GPIO2_23 29
GPIO0_10 31
GPIO0_9 33
GPIO0_8 35
GPIO2_14 37
GPIO2_12 39
GPIO2_10 41
GPIO2_8 43
GPIO2_6 45
2 DGND
4 GPIO1_7
6 GPIO1_3
8 GPIO2_3
10 GPIO2_4
12 GPIO1_12
14 GPIO0_26
16 GPIO1_14
18 GPIO2_1
20 GPIO1_31
22 GPIO1_5
24 GPIO1_1
26 GPIO1_29
28 GPIO2_24
30 GPIO2_25
32 GPIO0_11
34 GPIO2_17
36 GPIO2_16
38 GPIO2_15
40 GPIO2_13
42 GPIO2_11
44 GPIO2_9
46 GPIO2_27
P8
+5V
VDD_5V
DGND
GND
VDD_ADC
U1A
U1B
U1C
U1D
OPA4376
C1 100n
R1 1.8k
R2 1.8k
R3 1.8k
R4 1.8k
R5 29.4k
R6 29.4k
R7 29.4k
R8 29.4k
RTD1
RTD2
RTD3
RTD4
R9 200k
R10 200k
R11 200k
R12 200k
C6 500p
C7 500p
C8 500p
C9 500p
U2 INA326
U3 INA326
U4 INA326
U5 INA326
C2 0.1u
C3 0.1u
C4 0.1u
C5 0.1u
R13 100
R14 100
R15 100
R16 100
C10 1u
C11 1u
C12 1u
C13 1u
AIN0
AIN2
AIN4
AIN6
R17 4.7k
GPIO0_2
DS18B20_1
DS18B20_2
DS18B20_3
DS18B20_4
DS18B20_5
DS18B20_6
DS18B20_7
DS18B20_8
DS18B20_9
DS18B20_10
DS18B20_11
DS18B20_12
DS18B20_13
DS18B20_14
DS18B20_15
DS18B20_116
T1
T2
T3
T4
T5
T6
T7
T8
T9
T10
T11
T12
T13
T14
T15
T16
SSR1
SSR2
SSR3
SSR4
SSR5
SSR6
SSR7
SSR8
GPIO2_13
GPIO2_15
GPIO2_16
GPIO0_8
GPIO2_14
GPIO2_12
GPIO0_11
GPIO2_17
RELAY_1
RELAY_2
RELAY_3
RELAY_4
RELAY_5
RELAY_6
RELAY_7
RELAY_8
D1 LED
R34 90
HT1
HT2
H&T 1
H&T 2
R18 270
R19 270
U6A
U6B
OPA2376
C14 100n
R20 120k
R21 120k
R22 100k
R23 100k
AIN1
AIN3
AIN5
AIN7
JP1
JP2
Jumper_NC_Dual
+24V
DMT143_1
DMT143_2
DMT1
DMT2
R32 90
R33 90
SWITCH
12V/24V
12/24V1
S1
PWR1
EXT_PWR (+12/24)
GND1
U7 TPS54202H
VIN
EN
SW
BOOT
FB
GND
R29 510k
C15 0.1u
L1 15u
C16 22u
C17 22u
C18 75p
C19 10u
C20 0.1u
R28 69.8k
R30 100k
R31 33k
Sheet: /
File: TempBoard.sch
Title:
Size: A3
Date:
Rev:
KiCad E.D.A. kicad 4.0.6
Id: 1/1